

Real-Time Fuzzy Logic Control of Switched Reluctance Motor

Tarık ÜNLÜ¹, Ali UYSAL^{*1}

Accepted : 29/06/2017 Published: 30/09/2017

Abstract:In this study, 8/6 switched reluctance motor (SRM) is controlled by fuzzy logic. For driving SRM, four phase asymmetric bridge converter is chosen. STM32F4 Discovery processor and MATLAB Simulink software fuzzy logic controller (FLC) are used. SRM's speed and current are transferred to the computer in real-time. Measured speeds and currents are plotted. It is shown here that, the SRM for different reference speeds and loads is controlled by a STM32F4 Discovery card with MATLAB Simulink FLC.

Keywords:Switched reluctance motor, fuzzy logic, speed control, embedded system, PC-based

1. Introduction

Real-time performance of controllers takes a long process during industrial design. Depending on increased demands, the importance of designing real time controllers become crucial due to: 1) testing the system in real time, and 2) reducing project completion time [1].

Testing control techniques and evaluated their performance in real-time is critical issue for future controllers design. Fuzzy logic has been already successfully used in industrial applications. Especially, for modeling and controlling nonlinear systems fuzzy logic has an inevitable importance [2].

SRM is a nonlinear system which is the most important characteristic of SRM. The reason for this is a nonlinear inductance of magnetic circuit which is depending on phase current and rotor positions [3, 4]. Because of the nonlinear characteristic of the SRM and variable parameters, it needs a controller which is able to control SRM. To use classical controllers on a system, a mathematical model describing the system phenomena must be known. Because of this reason, the classic controllers such as P, PI, and PID controllers does not meet the requirements[5]. For SRM controlling, a nonlinear control system must be used [6]. In the last decades, intelligent control techniques are used for nonlinear system and also many studies are done on SRM speed controls by using intelligent techniques [7-10].

The MATLAB Simulink software is useful to use in real-time data exchange. Besides this, it is, also used in many control applications. For example, it is used for a dynamic system modeling, its simulation and analysis [11,12]. In the literature, numerous studies in real-time system control are performed with MATLAB/Simulink software [13-15].

Digital signal processors which are designed with fuzzy controllers using MATLAB are commonly used for real time applications. TMS, Spartan and Xilinx cards are the most common cards in academic studies [16-18]. Due to technological progress on microcontrollers, economic microcontrollers which

are compatible with MATLAB simulink, and have been developed recent decades, the STM32F4 Discovery microcontroller is one of this economic microcontroller [19, 20]. In this study, SRM was controlled by the fuzzy logical controlled driver. For driving SRM, we chose four phase asymmetric bridge converter. SRM's speed control was done by fuzzy logic and was controlled in real time using MATLAB Simulink software. In real time control, motor's current and speed outputs were transferred instantaneously to the computer and in the MATLAB Simulink software, the fuzzy logic controller was performed. MATLAB Simulink software is able to graph motor's speed and current values in real time.

Samples of fungal affected images are shown in (Figure.1 & 2).

2. Proposed Methodology

A block diagram for SRM's real time control is given in Fig. 1 and an experimental design for SRM's speed control are given in Fig. 2. In this study, 8/6 SRM is chosen to test the driver implemented. Technical specifications of SRM are given in the Table I. This motor is commonly used in mid-range industrial applications.

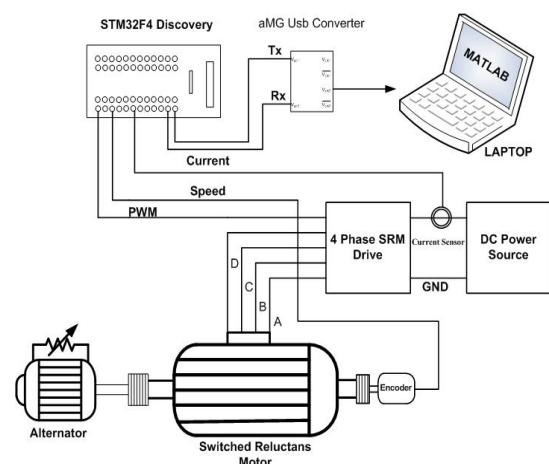


Figure1. Block diagram of test setup

Disregarding the common reluctance between phases, SRM's basic equivalent circuit can be written. The voltage applied to one phase can be defined as the sum of the voltage drop on the

¹ Department of Mech. Eng., Karabük University, Faculty of Technology, Karabük, 78050, Türkiye

* Corresponding Author: Email: aliuyosal@karabuk.edu.tr

winding resistance and the winding flux variation [21].

Table 1. Motor Technical Specifications.

Specifications	Value
Maximum Power	2.31 kW
Continuous Power	1.34 kW
Maximum Torque	3.4Nm
Continuous Torque	1.8Nm
Supply Voltage	96V
Rated speed	6000rpm
Phase impedance	10mΩ
$L_{aligned}$	2.06mH
$L_{unaligned}$	0.45mH

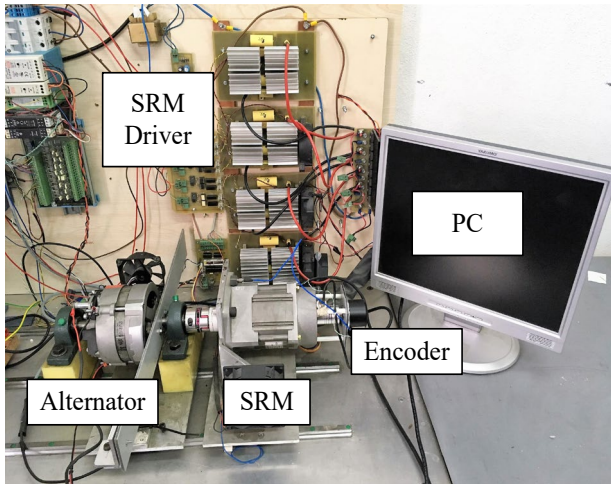


Figure 2. Test setup

SRM's phase equivalent circuit which is obtained from the voltage equation and electromotive force is given in Fig. 3. Electrical expression of one phase of SRM is given in equation (1).

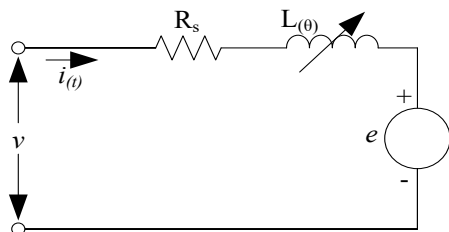


Figure 3. A phase equivalent circuit of the SRM.

$$V = R_s i + \frac{d\varphi(\theta, i)}{dt} \quad (1)$$

In equation (1), V is the supply voltage, R_s is winding resistance per phase, i is the current of phase (A), θ rotor position (rad), $L_{(\theta, i)}$ is the phase reluctance depending on rotor position and phase current, φ is magnetic flux. Magnetic flux equation is given in equation (2) and phase voltage equations are given in equations (3 and 4).

$$\varphi = L_{(\theta, i)} i \quad (2)$$

$$v = R_s i + \frac{d\{L_{(\theta, i)} i\}}{dt} = R_s i + L_{(\theta, i)} \frac{di}{dt} + \frac{dL_{(\theta, i)}}{d\theta} \frac{d\theta}{dt} \quad (3)$$

$$v = R_s i + L_{(\theta, i)} \frac{di}{dt} + \frac{dL_{(\theta, i)}}{d\theta} \omega_m i \quad (4)$$

In equation (4), $R_s i$ defines the ohmic voltage drop, $L_{(\theta, i)} \frac{di}{dt}$ defines an inductive voltage drop and $\frac{dL_{(\theta, i)}}{d\theta} \omega_m i$ represents induced electromotive force.

The instantaneous power equation (5) is obtained by putting winding flux in equation (1) and multiplying with current (i).

$$p_i = v i = R_s i^2 + i^2 \frac{dL_{(\theta, i)}}{dt} + L_{(\theta, i)} i \frac{di}{dt} \quad (5)$$

$$\frac{di}{dt} \left(\frac{1}{2} L_{(\theta, i)} i^2 \right) = L_{(\theta, i)} i \frac{di}{dt} + \frac{1}{2} i^2 \frac{dL_{(\theta, i)}}{dt} \quad (6)$$

The instantaneous power finally is written in equation (7) by putting p_i in equation (6).

$$p_i = v i = R_s i^2 + \frac{di}{dt} \left(\frac{1}{2} L_{(\theta, i)} i^2 \right) + \frac{1}{2} i^2 \frac{dL_{(\theta, i)}}{dt} \quad (7)$$

In equation (7), $R_s i^2$ represent a winding ohmic losses, $\frac{di}{dt} \left(\frac{1}{2} L_{(\theta, i)} i^2 \right)$ represent an exchange ratio in field energy and $\frac{1}{2} i^2 \frac{dL_{(\theta, i)}}{dt}$ represent an air gap power (pa).

A linear load is used for loading SRM and a synchronous alternator which is chosen. SRM's revolutions are obtained by an encoder. The current probe measures SRM's current values [22]. (360 pulse/round encoder is used to measure the rpm of SRM and 20A measuring ranged current sensor is used to measure the current of the SRM [22].)

The STM32F4 Discovery card is used for motor speed control in this study. STM32F4 Discovery is preferred in robotics, embedded systems, and many platforms. It is compatible with MATLAB Simulink software. It can also have a real-time application feature. The most important advantage of this card is a low cost comparing with the similar cards. It is easily obtainable and commonly used for many applications. (Controller produces 1 kHz digital output signal.)

2.1. Method

To apply a fuzzy logic controller (FLC) on a system, firstly system's input and output must be determined. The FLC's input and output variables are given in Fig. 4. An error on motor speed and an error ratio are chosen as an input variable. The motor speed error and error ratio equations are given in equation (8) and (9) respectively.

$$e_\omega(k) = \omega^* - \omega(k) \quad (8)$$

$$ce_\omega(k) = e_\omega(k) - e_\omega(k-1) \quad (9)$$

In equation (8), ω^* is a reference speed, $\omega(k)$ is a real speed obtained from the motor, $e_\omega(k)$ is speed error and $e_\omega(k-1)$ is previous speed error.

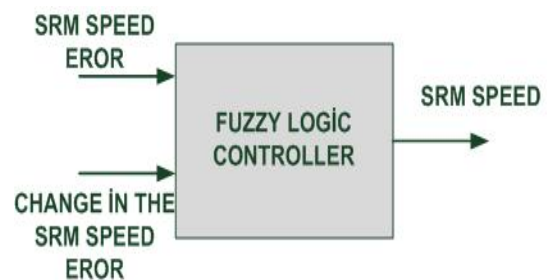


Figure 4. Input-Output Variables.

Table 2. Rule Base Table.

$\frac{ce_{\omega}}{e_{\omega}}$	NB	NM	NS	ZE	PS	PM	PB
NB	NB	NB	NB	NB	NM	NS	ZE
NM	NB	NB	NB	NM	NS	ZE	PS
NS	NB	NB	NM	NS	ZE	PS	PM
ZE	NB	NM	NS	ZE	PS	PM	PB
PS	NM	NS	ZE	PS	PM	PB	PB
PM	NS	ZE	PS	PM	PB	PB	PB
PB	ZE	PS	PM	PB	PB	PB	PB

In this study, FLC’s rule base is given as:

IF $e_{\omega}(k)=PB$ AND $ce_{\omega}(k)=PS$ THEN $\Delta(i)=NB$ [23]

IF $e_{\omega}(k)=NB$ AND $ce_{\omega}(k)=NM$ THEN $\Delta(i)=NB$

IF $e_{\omega}(k)=NB$ AND $ce_{\omega}(k)=NS$ THEN $\Delta(i)=NB$

In the rule base, for VE function, $e_{\omega}(k)$ and $ce_{\omega}(k)$ inputs define Mamdani’s minimum rule. Converting fuzzy output values to digital values, a weighted centroid method is used.

$$z^* = \frac{\int \mu_{\underline{C}}(z).zdz}{\int \mu_{\underline{C}}(z)dz} \quad (10)$$

In equation (10) \underline{C} represents the union of output function and z represents the membership values.

MATLAB Simulink model in Fig. 6 is performed for SRM’s speed control by FLC. In the model, FLC’s input-output values and a rule base is transferred to MATLAB using the MATLAB FIS editor.

For FLC input variables $e_{\omega}(k)$ and $ce_{\omega}(k)$, membership functions are given in Fig. 7 and Fig. 8. For both input variables, 7 labeled membership functions are used. Here NB(Negative Big), NM(Negative Medium), NS(Negative Small), ZE(Zero), PS(Positive Small), PM(Positive Medium) and PB(Positive Big) labels are defined.

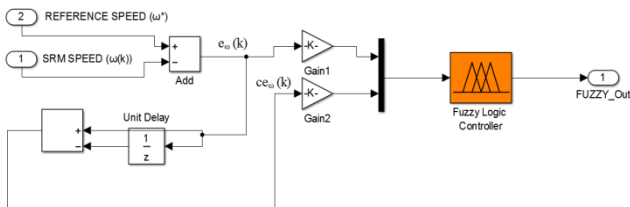


Figure 5.Input-output Variables.

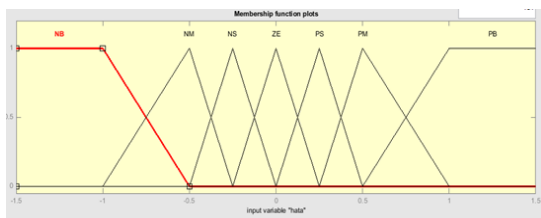


Figure 6. $e_{\omega}(k)$ membership function.

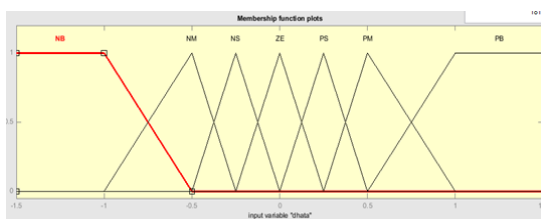


Figure 7. $ce_{\omega}(k)$ membership function.

There is a one FLC’s output variable $\Delta(i)$. A membership function of the output variable is given in Fig. 9. For Output

variable, NS(Negative Big), NM(Negative Medium), NS(Negative Small), ZE(Zero), PS(Positive Small), PM(Positive Medium) and PB(Positive Big) labels are used. The membership functions belonging to the input and the output variables are obtained by trial and error method.

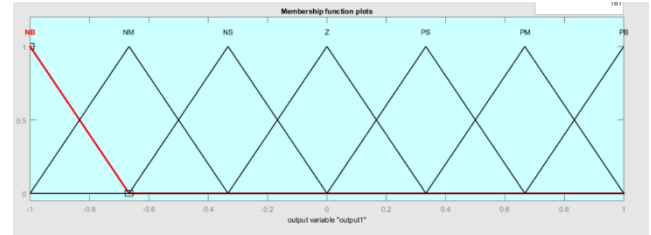


Figure 8.Output value membership function.

3. Results and Discussion

Performed unload, quarter loaded and half-loaded experiment’s measurements are transferred to MATLAB and graphs are plotted in MATLAB.

SRM is investigated for different motor speeds and loads. 1500 rpm and 3000 rpm motor speeds were used in this study.

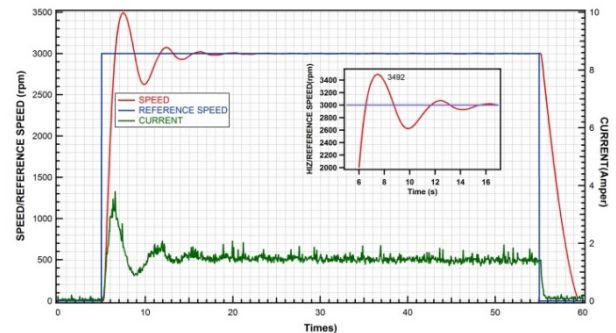


Figure 9.No load (0Nm) at 3000rpm speed graphic of SRM.

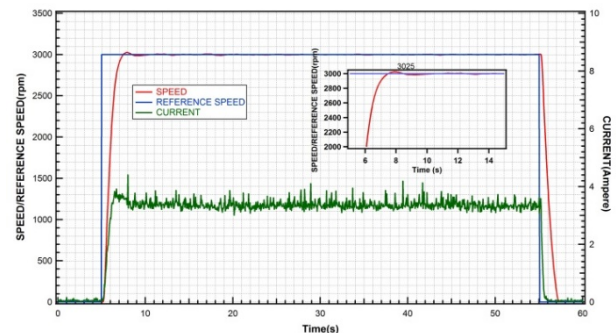


Figure 10.Quarter load (0.4Nm) at 3000rpm speed graphic of SRM.

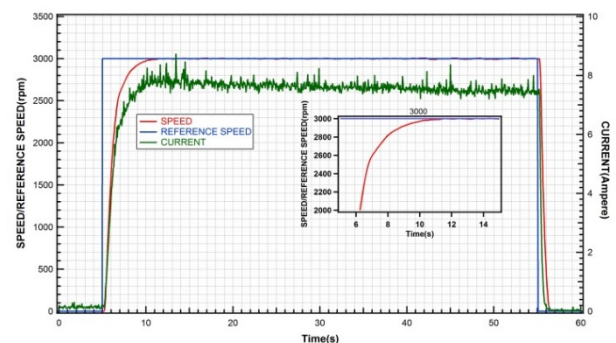


Figure 11.Halfload(0.9Nm) at 3000rpm speed graphic of SRM.

Depending on the load situation, different SRM’s responses were observed. For unloaded (Fig. 10) and quarter loaded SRM (Fig.

11), overflows were observed, before reaching steady level, besides those for half-loaded SRM, overflows did not observe (Fig. 12). Overflow rate was calculated 16 % for unloaded SRM, 1% for quarter loaded SRM. The lowest rise time was observed for unloaded SRM, the highest rise time was observed for half-loaded SRM. Rise-time and overflow time were tabulated in Table 3. When the SRM's speed reach follow the reference speed, the current decrease was also observed. During first speed up, the current was measured as 2.6 A, 4 A, 7.2 A. When the SRM reaches the steady state, the current was also stable.

Table 3. Unloaded, quarter load, half load results

Motor Load Status	Rise Time (t)	Peak Time (t _p)	Settling Time (t _s)	Max. Overshoot (rpm)	Error Rate (%)
Unloaded	1.5 s	2.4 s	6.4 s	492	16
Quarterload	2.5 s	2.9 s	5.4 s	25	1
Halfload	5.2 s	-	5.2 s	-	-

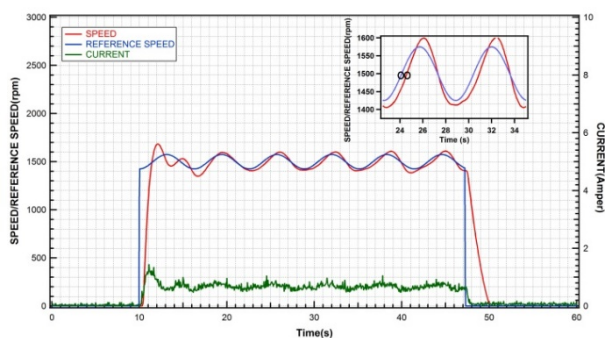


Figure 12. No load (0Nm) sinus at 1500 rpm speed graphic of SRM.

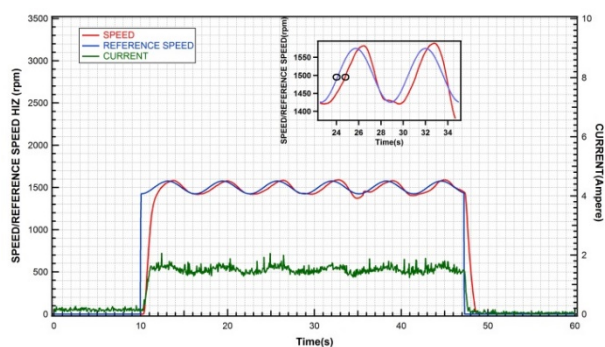


Figure 13. Quarter load (0.4Nm) sinus at 1500 rpm speed graphic of SRM

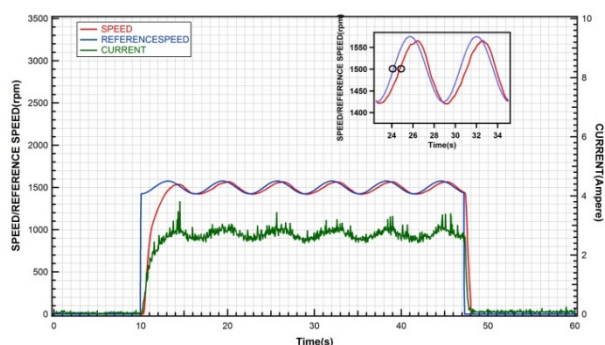


Figure 14. Halfload (0.9Nm) sinus at 1500 rpm speed graphic of SRM.

1500 rpm motor speed with applied sinus function, graphs for unloading SRM (Fig. 13), quarter-loaded SRM (Fig. 14) and half-loaded SRM (Fig. 15) is plotted. The Phase difference between SRM's measured speed and reference speed for unloading, quarter-loaded and half-loaded are measured of 25°, 40° and 42°, respectively.. While SRM's measured speed is following the

reference speed, and the current is also observed as follows a sinus wave.

4. Conclusion

In this study, the control of SRM is done at different speed and load levels. The target-host method is applied successfully. The equipments used in the study are cheap and their accessibility is easy, which provided a significant advantage on this study. Experimental studies showed that SRM runs effectively via fuzzy logic control under different conditions. The reference speed applied to the motor is caught and steady state is provided. The real-time control used in this study can be applied to other studies, condition monitoring and fault diagnosis studies.

Acknowledgements

Project (No. KBÜ-BAP-C-11-D-003) supported by the Karabük University BAP Unit,

References

- [1] Ö. A. TEKİN (2007). Implementation of real-time fuzzy controllers. M.S. thesis, Dept. Electron. Eng., İstanbul Teknik Univ., İstanbul, Turkey.
- [2] A. L. Zadeh (1965). Fuzzy sets information and control. *World Scientific* Publishing, New York. Pages. 339–353.
- [3] R. Krishanan (2011). Switched reluctance motor drives: Modeling Simulation, Analysis, Design and Applications., CRC Press.
- [4] O. F. Bay and C. Elmas (2013). Modeling of the inductance variation and control of the switched reluctance motor based on fuzzy logic. *Intelligent Automation and Soft Computing*, vol. 10, Pages. 233–246.
- [5] Ç. Elmas, M. A. Akçayol and T. Yiğit (2007). Fuzzy PI controller for speed control of switched reluctance motor. *J. Fac. Eng. Arch. Gazi Univ.*, Vol. 22. Pages. 65–72.
- [6] E. Karakas and S. Vardarbası (2007). Speed control of SR motor by self-tuning fuzzy PI controller with artificial neural network. *Sadhana*, Vol. 32. Pages. 587–596.
- [7] S. Paramasivam and R. Arumugam (2005). Hybrid fuzzy controller for speed control of switched reluctance motor drives. *Energy Conversion and Management*. Vol. 46. Pages. 1365–1378.
- [8] M. A. Akçayol and C. Elmas (2005). NEFCLASS-based neuro-fuzzy controller for SRM drive. *Engineering Applications of Artificial Intelligence*. Vol. 18. Pages. 595–602.
- [9] B. M. Dehkordi, A. Passapoor, M. Moallem and C. Lucas (2011). Sensorless speed control of switched reluctance motor using brain emotional learning-based intelligent controller. *Energy Conversion and Management*. Vol. 52. Pages. 85–96.
- [10] E. Daryabeigi and B. M. Dehkordi (2014). Smart bacterial foraging algorithm based controller for speed control of switched reluctance motor drives. *International Journal of Electrical Power & Energy Systems*, vol. 62, pp. 364–373, 2014.
- [11] M. J. Er, M. T. Lim and H. S. Lim (2001). Real-time hybrid adaptive fuzzy control of an SCARA robot. *Microprocessor and Microsystems*. Vol. 25. Pages. 369–378.
- [12] H. Açıkgöz, Ö.F. Keçecioglu, A. Gani and M. Şekkelı (2014). Speed control of direct torque controlled induction motor by using PI, anti-windup PI and fuzzy logic

controller. *International Journal of Intelligent Systems and Applications in Engineering*. Vol. 2. Pages. 58-63.

- [13] H.R. Jayetileke, W.R. de Meland, H.U.W. Ratnayake (2014). Real-time fuzzy logic speed tracking controller for a DC motor using Arduino Due. In *Conf. Rec. 2014 IEEE Int. Conf. Information and Automation for Sustainability*. Pages. 22–24.
- [14] P. Bhatkhande and T. C. Havensand (2014). Real-Time Fuzzy Controller For Quadrotor Stability Control. In *Conf. Rec. 2014 IEEE Int. Conf. on Fuzzy Systems*. Pages. 913–919.
- [15] S. Paramasivam and R. Arumugam (2005). Real-time DSP-based adaptive controller implementation for 6/4 pole switched reluctance motor drive. *Songklanakarin J. Sci. Technol.* Vol. 27. Pages. 523–534.
- [16] E. A. E. M. Ramadan, M. El-Bardini, N. M. El-Rabaie and M. A. Fkirin (2014). Embedded system based on a real-time fuzzy motor speed controller. *Ain Shams Engineering Journal*. Vol. 5. Pages. 399–409.
- [17] M. A. Akçayol (2004). Application of adaptive neuro-fuzzy controller for SRM. *Advances in Engineering Software*. Vol. 35. Pages. 129–137.
- [18] I. Koyuncu (2016). Design and implementation of high speed artificial neural network based Sprott 94 S system on FPGA. *International Journal of Intelligent Systems and Applications in Engineering*. Vol. 4. Pages. 33-39.
- [19] D. S. Reay (2014). Hands-on real-time teaching using inexpensive ARM Cortex M4 development systems. In *Conf. Rec. 2014 IEEE Int. Conf. on Acoustic, Speech and Signal Processing*. Pages. 2224–2227.
- [20] İ. İlhan (2016). Solution for the travelling salesman problem with a microcontroller-based instantaneous system. *International Journal of Intelligent Systems and Applications in Engineering*. Vol. 4. Pages. 122-127.
- [21] T. J. E. Miller, J. M. Stephenson, S. R. Macminn and J.R. Handersot (2004). *Switched reluctance drives*. IEEE Industry Applications Society. Tutorial Course.
- [22] E. Soylu and R. Bayir (2016). Measurement of Electrical Conditions of Rechargeable Batteries. *Meas. Control*. Vol. 49. Pages. 72–81.
- [23] C. C. Lee (1990). Fuzzy logic in control systems: Fuzzy logic controller, Part II. *IEEE Transactions on Systems, Man and Cybernetics*. Vol. 20. Pages. 419–435.